

## Increased phase synchronization of spontaneous calcium oscillations in epileptic human versus normal rat astrocyte cultures

Gábor Balázs

*Center for Neurodynamics, University of Missouri at St. Louis, St. Louis, Missouri 63121*

Ann H. Cornell-Bell

*Viatech Imaging, Ivoryton, Connecticut 06442*

Frank Moss

*Center for Neurodynamics, University of Missouri at St. Louis, St. Louis, Missouri 63121*

(Received 28 October 2002; accepted 26 February 2003; published 7 May 2003)

Stochastic synchronization analysis is applied to intracellular calcium oscillations in astrocyte cultures prepared from epileptic human temporal lobe. The same methods are applied to astrocyte cultures prepared from normal rat hippocampus. Our results indicate that phase-repulsive coupling in epileptic human astrocyte cultures is stronger, leading to an increased synchronization in epileptic human compared to normal rat astrocyte cultures. © 2003 American Institute of Physics.

[DOI: 10.1063/1.1567652]

**In classical thermodynamics, coupling helps isolated linear systems to reach equilibrium by erasing spatial nonuniformities and thereby increasing their entropy.<sup>1</sup> In nonlinear systems, such as the Belousov–Zhabotinsky chemical reaction,<sup>2,3</sup> astrocyte cultures,<sup>4</sup> and bacterial colonies,<sup>5</sup> coupling allows for propagation of the nonequilibrium state in the form of waves or synchronized oscillations.<sup>6</sup> The laws governing the biological world, however, include competition (inhibition) whereby spatial nonuniformities are amplified. We show that calcium oscillations in epileptic astrocyte cultures provide an example for this latter case, that is their coupling is inhibitory. Moreover, we define two new measures that characterize the cultures: the first quantifies the intensity of oscillations in the culture, while the second quantifies the strength of coupling between cells. We show that both of these measures have high values in epileptic human astrocyte cultures when compared with those obtained from normal rat brain. Whether the modified properties of the astrocyte network are a cause or an effect of epilepsy is an open question.**

Glial cells induce and stabilize synapses, affect synaptic plasticity and integrate neuronal inputs, thus having become a subject of intense study.<sup>7,8</sup> They are also essential to the pathology of the nervous system.<sup>9</sup> Glial activity can be monitored through the variations of free intracellular calcium concentration ( $[Ca^{2+}]_i$ ).

To date studies of astrocyte  $Ca^{2+}$  dynamics have focused on waves<sup>10</sup> and oscillations.<sup>11</sup> Diffusion of chemical agents across gap junctions and through extracellular space have been attributed an equally significant role in the propagation of  $Ca^{2+}$  waves.  $Ca^{2+}$  oscillations are, however, intracellular phenomena: by definition, they do not propagate or influence the  $Ca^{2+}$  activity of other cells.

Here we apply methods introduced by Balázs *et al.*<sup>11</sup> to

spontaneous  $Ca^{2+}$  oscillations in 45 human astrocyte cultures (recorded in normal saline), and compare the outcome with the results of the same analysis applied to three normal rat hippocampal cultures. Two measures of the astrocyte network behavior are introduced during our analysis: the *oscillation intensity A* and the *degree of synchronization K* between oscillators. By definition, the oscillation intensity has a high value for a high density of  $Ca^{2+}$  oscillators with high frequency of oscillation. The degree of synchronization measures the interaction between individual oscillators (it has a high value if all the oscillators synchronize their activities). The degree of synchronization might be related to, but is not equivalent with connectivity due to physical coupling of cells through gap junctions.

Temporal lobectomy was performed on three patients suffering of incurable epilepsy.<sup>12</sup> Three tissue samples from five brain areas (amygdala, cortex, hippocampus, parahippocampus and the uncus of the parahippocampus) were obtained from each patient following surgery. Astrocyte cultures were prepared from regions of the brain that correlated to hyperexcitable EEG in the operating room.<sup>13</sup> After purification, 45 astrocyte cultures resulted with high purity of cell lineage. The cultures were maintained in normal saline. Three samples of normal rat hippocampus were prepared using the same method, and served as control in our analysis.

For  $Ca^{2+}$  imaging, the astrocyte culture was placed in a flow-through perfusion chamber and was stained using a calcium-sensitive dye, Fluo3-AM ( $2 \mu M$ ). The properties of the dye permit visualization of calcium ion concentration (the dye is fluorescent in the presence of free calcium ions and the fluorescence increases with the concentration of free calcium). The culture was washed out in normal saline while the dye remained present inside the astrocytes. Next, the probe was placed under a confocal scanning laser microscope (BioRad MRC 500/600). Fluorescence images were collected every 1.8 seconds using the frame grabber board on the computer (Panasonic 3031TQ). Images were downloaded

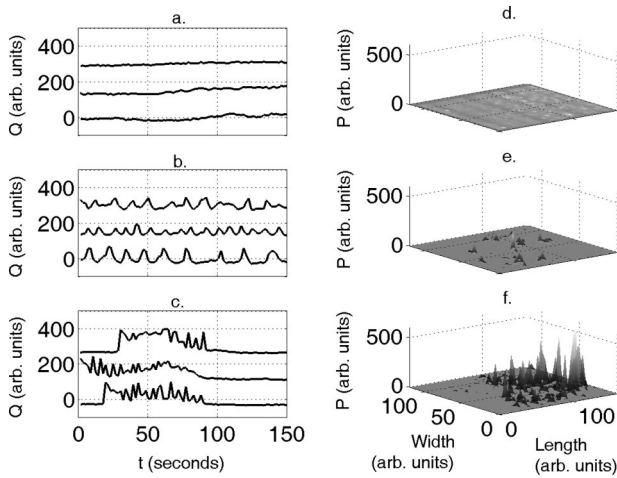


FIG. 1. Time series and power ( $P_{ij}$ ) maps for the three example image series. (a), (b), (c) Time series of the three oscillators with highest power  $P_{ij}$  from image series 1, 2, and 3, respectively; (d), (e), (f) maps of power  $P_{ij}$  for image series 1, 2, and 3, respectively.  $Q_i$  (the grayscale value) is a number approximately proportional to the local  $Ca^{2+}$  concentration. The values of oscillation intensity  $A = \langle P_{ij} \rangle$  are 4.14, 106.32, and 407.16 from top to bottom.

directly to an optical memory disk recorder. Finally, the results were stored as  $480 \times 640$  pixel grayscale images, every pixel's values ranging from 0 to 255 (corresponding to black and white, respectively). In these images, two pixels typically correspond to one micron. The size of a typical astrocyte is 10–20 microns.

To reduce the high spatial and temporal noise affecting the image series, the resolution of the images was reduced by computing averages over  $11 \times 11$ -pixel squares centered at every fourth pixel, both horizontally and vertically. Thus, the resulting image series contained  $120 \times 160$  pixel grayscale images. The values around the borders were set to 0 to eliminate border effects and the digital text created by the camera. The resulting image series typically contained 100 images taken 1.8 seconds apart.

We choose three preprocessed image series to illustrate the application of our computational measures  $A$  and  $K$ . In the first image series (called “1”) the cells show almost no  $Ca^{2+}$  activity; in the second (called “2”) several cells show  $Ca^{2+}$  oscillations; finally, in the last (called “3”) a large number of cells show very intense oscillatory activity. The time series of the grayscale values of three typical cells in the image series are shown in Figs. 1(a)–1(c).

To identify the position  $(i, j)$  of rapidly oscillating astrocytes, we developed a computational measure, in analogy to the definition of power in alternating current (ac) circuits defined as

$$P = R \langle I^2(t) \rangle = \frac{R}{\tau} \int_0^\tau \left[ \frac{dQ}{dt} \right]^2 dt,$$

where  $I$  is the value of the current at time  $t$ ,  $Q$  is the electric charge,  $R$  is the resistance of the circuit,  $\tau$  is the duration of the measurement and  $\langle \cdot \rangle$  denotes temporal average. Similarly, the power  $P_{i,j}$  at a specific location in the image series is defined by the discretization of the previous formula:

$$P_{i,j} = \frac{1}{N_F(\Delta t)^2} \sum_{t=\Delta t}^\tau [Q_{i,j}(t) - Q_{i,j}(t - \Delta t)]^2,$$

where  $Q_{i,j}$  is the grayscale value at position  $(i, j)$ ,  $R = 1$ ,  $\Delta t = 1.8$  seconds is the time interval between two consecutive frames, and  $N_F$  is the total number of frames. We calculate the intensity  $A$  by averaging the power measured at the 10 positions with maximum power:  $A = \langle P_{i,j} \rangle$ . The maps of power  $P_{i,j}$  for the three image series are shown in Figs. 1(d)–1(f). Notice that  $A$  increases with the number of oscillators with high frequency and amplitude (4.14, 106.32, and 407.16 from top to bottom).

Next, we define the degree of synchronization  $K$  based on stochastic phase synchronization.<sup>14</sup> By definition, two oscillators are synchronized (or phase-locked) if the difference of their phases tends to a constant. Therefore, first we define the time-dependent phase at each point in the image. This definition is based on marker events, which are the peaks of  $[Ca^{2+}]_i$ . Typically, we find the peaks based on the following procedure: we first subtract a running average from the time series  $Q_{i,j}(t)$  at every position  $(i, j)$ , and then impose the condition that the difference  $2Q_{i,j}(t) - Q_{i,j}(t - \Delta t) - Q_{i,j}(t + \Delta t)$  be larger than a threshold. Once the times when these  $[Ca^{2+}]_i$  peaks occur are found, the phase at position  $(i, j)$  is defined as

$$\phi_{i,j}(t) = 2\pi \frac{t - t_{i,j}^{(k)}}{t_{i,j}^{(k+1)} - t_{i,j}^{(k)}} + 2k\pi,$$

where  $t_{i,j}^{(k)}$  denotes the time when the  $k$ th marker event (peak) occurs at position  $(i, j)$ . Taking the phases at two locations  $(i_0, j_0)$  and  $(i, j)$ , the wrapped phase difference is defined as  $\Phi_{i_0, j_0; i, j}(t) = [\phi_{i_0, j_0}(t) - \phi_{i, j}(t)]_{\text{mod}(2\pi)}$ , with values always in  $[-\pi, \pi]$ . If this interval is divided into  $N_B$  equal-size bins, it becomes possible to define the probability  $p_n$  for the phase difference to fall into the  $n$ th bin. The distribution of phase differences for two example pairs of oscillators from the image series is shown in Figs. 2(a)–2(c). Notice that the prominence of the peaks in the distributions increases from image series 1 to 2 and then to 3. Prominent peaks are an indication of phase locking.

To quantify how “peaky” a distribution is, we use the synchronization index (SI) defined for positions  $(i_0, j_0)$  and  $(i, j)$  as

$$\rho = \frac{S_{\max} - S_{i_0, j_0; i, j}}{S_{\max}},$$

where  $S_{i_0, j_0; i, j} = -\sum_{n=1}^{N_B} p_n \log_2(p_n)$  is the Shannon entropy associated with the probability distribution of the phase difference.  $S_{\max}$  is the Shannon entropy of a completely flat distribution over  $N_B$  bins,  $S_{\max} = \log_2(N_B)$ . The SI maps for the image series are shown in Figs. 2(d)–2(f).

To define the degree of synchronization  $K$ , we select the 10 oscillators with the highest power  $P_{i,j}$  (the most elevated peaks in Fig. 1), and calculate the SI between every possible pair of locations, never taking the same pair twice. These SI's are spatial averages taken within small regions surrounding the chosen pair of sites. Thus we obtain 45 average

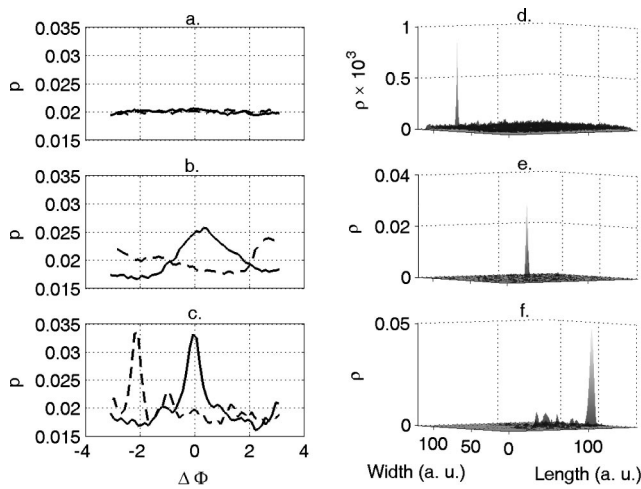


FIG. 2. Phase difference probability distributions (left) and synchronization index maps (right) for the three example image series. (a), (b), (c) Distribution of the phase difference  $\Delta\Phi$  for two pairs of oscillators, for image series 1, 2, and 3, respectively; (d), (e), and (f) synchronization index ( $S_{i_0, j_0; i_j}$ ) maps for three image series 1, 2, and 3, respectively. An oscillator with high power  $P_{i_0, j_0}$  is located at position  $(i_0, j_0)$ , and the SI's of all the other positions  $(i, j)$  in the image series are shown with respect to  $(i_0, j_0)$ . Dashed and solid lines in (a), (b), and (c) refer to two different pairs of cells. One pair of astrocytes oscillate in phase (solid line), indicating phase-attractive coupling as shown by the maximum at  $\Delta\phi \approx 0$ . The other pair of cells oscillate in antiphase (dashed line), indicating phase-repulsive coupling, as shown by the maxima at  $\Delta\phi \approx \pm\pi$ . The degrees of synchronization  $K$  are 0.000 027, 0.000 716, and 0.001 924, from top to bottom.

SI values for 45 pairs of positions, from which we finally determine the degree of synchronization  $K$ , defined as the average of all 45 SI's:  $K = \langle \rho_{i_m, j_m; i_n, j_n} \rangle$ .

In Fig. 3 we show how the degree of synchronization  $K$  depends on the oscillation intensity  $A$  for all 48 different cultures. Image series 1, 2, and 3 are represented by gray triangles; the control (rat) image series are represented by

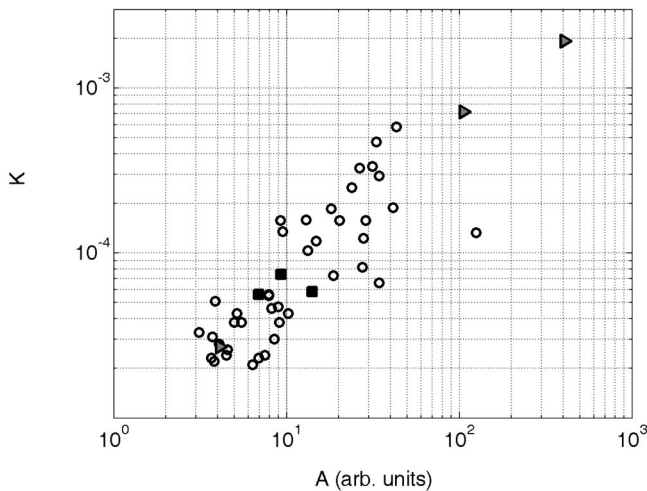


FIG. 3. Dependence of the degree of synchronization,  $K$ , upon the oscillation intensity  $A$  for all 48 image series. The image series with higher intensity  $A$  tend to also have higher degree of synchronization  $K$ . The meaning of symbols are gray triangles, the three example image series; black squares, the three control image series; empty circles, the remaining 42 image series. The correlation between the axes is 0.92.

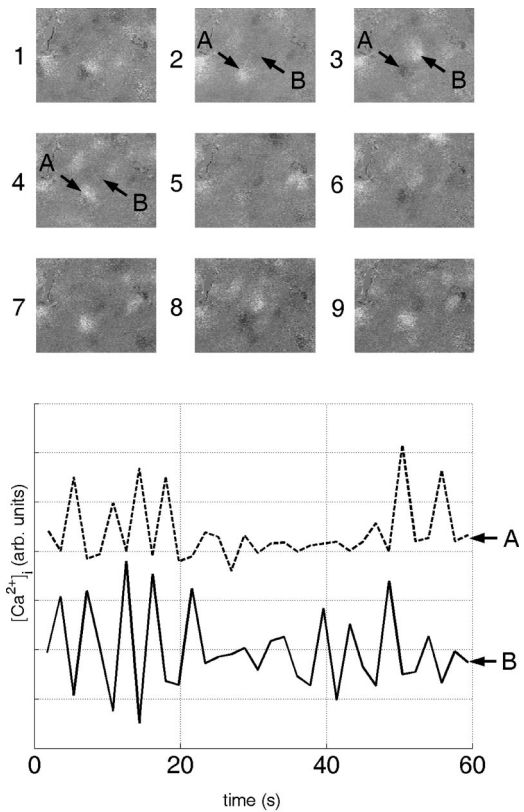


FIG. 4. Phase-repulsive coupling of intracellular  $Ca^{2+}$  oscillations in image series 3. Top, temporal image sequence of calcium oscillations in an epileptic astrocyte culture. Time is increasing from image 1 through image 9, time between frames is 1.8 seconds. Notice that  $[Ca^{2+}]_i$  time series of the two cells  $A$  and  $B$  oscillating in antiphase. Bottom:  $[Ca^{2+}]_i$  time series of the two cells  $A$  and  $B$  oscillating in antiphase.

black squares; empty circles represent the remaining 42 image series. Notice that the degree of synchronization  $K$  increases with the intensity of oscillations  $A$ .

The fact that elevated intensity implies high synchronization means that in tissue cultures with an increased number of high-power  $Ca^{2+}$  oscillators the coupling strength among astrocytes is increased. This coupling is, however, not of the usual type that accounts for the spreading of  $Ca^{2+}$  waves, which results from phase-attractive coupling, (i.e., the elevated  $[Ca^{2+}]_i$  induces the increase of  $[Ca^{2+}]_i$  in neighboring cells). The opposite situation is observable in image series 3, where a compactly packed group of powerful oscillators is present, occupying more than half of the image area (see Fig. 4 for a temporal sequence of a magnified portion). When a single cell or subgroup of cells have low  $[Ca^{2+}]_i$ , a neighboring cell or group have high  $[Ca^{2+}]_i$ , indicating that they oscillate in antiphase. This is a signature of phase-repulsive coupling (see Fig. 4 for an example, where the arrows indicate this behavior).

Our results indicate that epileptic astrocyte cultures exhibit substantial differences in calcium signaling when compared to normal cultures. Moreover, our measures  $A$  and  $K$  make it possible to quantify this. The intensity can be associated with culture pathology. It was previously shown that cultures originating from patients with intractable medial temporal lobe epilepsy have an increased number of sponta-

neous  $\text{Ca}^{2+}$  oscillators.<sup>9</sup> This means that the number of sites with high power  $P_{i,j}$  is considerably larger in the epileptic cultures compared with normal ones. Therefore, the oscillation intensity  $A$  is also larger, and thus is a direct measure of how pathologic the astrocyte culture is.

High values of oscillation intensity  $A$  imply increased degree of synchronization  $K$ , according to Fig. 4. Therefore, the degree of synchronization  $K$  is an alternate measure of pathology. Intracellular  $\text{Ca}^{2+}$ -oscillations synchronize in epileptic astrocyte cultures, unlike in normal cultures.<sup>15</sup> This implies again that epileptic astrocyte cultures are different from normal cultures. This conclusion is important, because it suggests a possible role for the astrocyte network in the initiation of seizures. Until now, the main focus was on neurons in attempts to determine the cause of epilepsy. Taking into account the bilateral interaction between neurons and glia,<sup>7,8</sup> and the fact that epileptic glia change their properties, it is reasonable to suspect that the astrocyte network plays an important role in rendering certain brain areas epileptic.

While the mechanisms leading to calcium wave propagation have been a subject of study, and have been reasonably well understood on the basis of phase-attractive coupling, nothing is known about how the intracellular  $\text{Ca}^{2+}$  dynamics of two astrocytes influence each other. The probability distributions of the phase differences [see Figs. 2(b) and 2(c)], however, imply that the interaction between neighboring astrocytes is phase-repulsive (dashed lines). The mediator of this interaction could be a biochemical agent diffusing through gap junctions and/or extracellular space, resulting in the mutual inhibition of  $\text{Ca}^{2+}$  oscillators. The fact that epileptic astrocytes show increased gap-junctional coupling when compared to normal cells,<sup>13</sup> however, seems to suggest that the route taken by the inhibitory agent is through gap junctions. The identification of this coupling agent remains an important open question for biochemistry.

In conclusion, our quantitative analysis of  $\text{Ca}^{2+}$  oscillations reveals specific alterations in  $\text{Ca}^{2+}$  signaling in epileptic human astrocytes cultures compared with normal rat cultures, and demonstrates a way to rigorously differentiate epileptic and healthy tissues. For example, one can set a

threshold in  $A$  or  $K$ , above which the tissues are epileptic. Further studies are needed in order to determine this threshold. Whether the modified properties of the astrocyte network are a cause or effect of epilepsy remains an open question.

## ACKNOWLEDGMENTS

We acknowledge support by the Graduate School at the University of Missouri, St. Louis (G.B.), the Office of Naval Research, Physics Division (G.B. and F.M.) and by an NIEHS SBIR phase II grant (ESO 8470-04) (A.H.C.-B.). We thank Alexander Neiman for discussions and Enrico Simonotto for programming. Surgery was performed by Nayef Al-Rodhan.

<sup>1</sup>K. R. Atkins, *Physics*, 2nd ed. (Wiley, New York, 1965), p. 223.

<sup>2</sup>P. Jung, A. Cornell-Bell, F. Moss, S. Kádár, J. Wang, and K. Showalter, *Chaos* **8**, 567–575 (1998).

<sup>3</sup>S. Kádár, J. Wang, and K. Showalter, *Nature (London)* **391**, 770–772 (1998).

<sup>4</sup>A. H. Cornell-Bell, S. M. Finkbeiner, M. S. Cooper, and S. J. Smith, *Science* **247**, 470–474 (1990).

<sup>5</sup>E. O. Budrene and H. C. Berg, *Nature (London)* **349**, 630–633 (1991).

<sup>6</sup>A. Neiman, L. Schimansky-Geier, A. Cornell-Bell, and F. Moss, *Phys. Rev. Lett.* **83**, 4896–4899 (1999).

<sup>7</sup>P. G. Haydon, *Nature Reviews Neuroscience* **2**, 185–193 (2001).

<sup>8</sup>E. M. Ullian, S. K. Sapperstein, K. S. Christopherson, and B. A. Barres, *Science* **291**, 657–664 (2001).

<sup>9</sup>A. H. Cornell-Bell and A. Williamson, in *Biology and Pathology of Astrocyte-Neuron Interactions*, edited by S. Fedoroff (Plenum, New York, 1993), pp. 51–65.

<sup>10</sup>P. Jung, A. Cornell-Bell, K. S. Madden, and F. Moss, *J. Neurophysiol.* **79**, 1098–1101 (1998).

<sup>11</sup>G. Balázsi, A. H. Cornell-Bell, A. Neiman, and F. Moss, *Phys. Rev. E* **64**, 041912 (2001).

<sup>12</sup>D. D. Spencer, in *Contemporary Issues in Neurological Surgery*, edited by S. Spencer and D. D. Spencer (Blackwell Scientific, Boston, MA, 1991), pp. 129–137.

<sup>13</sup>S. H. Lee, S. Magge, D. D. Spencer, H. Sontheimer, and A. H. Cornell-Bell, *Glia* **15**, 195–202 (1995).

<sup>14</sup>A. Pikovsky, M. Rosenblum, and J. Kurths, *Synchronization: A Universal Concept in Nonlinear Sciences* (Cambridge University Press, Cambridge, MA, 2001).

<sup>15</sup>A. H. Cornell-Bell and S. M. Finkbeiner, *Cell Calcium* **12**, 185–204 (1991).